объединенный
институт
ядерных
исследований
дубна

E2-84-313

V.P.Gerdt, A.S.Ilchev, V.K.Mitrjushkin,
I.K.Sobolev, A.M.Zadorozhny

PHASE STRUCTURE OF THE SU(2) LATTICE GAUGE-HIGGS THEORY

Submitted to "Nuclear Physics B"

1984

1. INTRODUCTION

The formulation of gauge theories on a space-time lattice [1] provided large possibilities for studying these theories beyond the scope of perturbation theory. The space-time lattice introduced into the physical (continuous) space-time allows us to find a nonperturbative regularization of ultraviolet divergences and to use powerfull numerical methods.

Of a special interest in lattice gauge theories is the study of phase diagrams. There are two arguments for the study of the phase structure of lattice theories. The first is the question of existence of a continuum limit of lattice theories. According to modern ideas [2] we may expect the continuum limit at the critical point, i.e., at the point of the second-order phase transition. The lattice action, as a rule, does not depend on the lattice spacing a explicitly but depends on "bare" interaction constants $(g_0(a), \lambda(a),...)$ and "bare" masses $(m_0(a))$ the dependence of which on the lattice spacing a is not known.

At the same time from general considerations it follows that the correlation length ξ in a lattice (in a units) system and lattice spacing a are related by [2] $a \sim 1/\xi(g_0, \lambda_0, m_0)$.

At the critical point of the lattice system the correlation length tends to infinity and the lattice spacing tends to zero. The continuum limit of (gauge-invariant) vacuum expectation values does exist if the critical behaviour is determined by a fixed point of the renormalization group. In the vicinity of this point a continuum field theory with an infinite cut-off may be defined.

There may exist several or even an infinite number of critical points of the lattice system. The existence of the two fixed points would mean the existence of two distinct continuum field theories and two distinct sets of critical exponents. The analysis of a continuum limit of some lattice gauge-Higgs models with frozen radial degree of freedom was done in [3,4].

The analysis of phase diagrams of gauge theories and search of critical points can supply us with good opportunity to study the continuum limit of lattice theories.

Second, the study of the phase structure of theories of gauge fields interacting with matter fields may help us to examine the problem of complementarity principle. According to the so-called complementarity principle [5,6], in the theory of gauge

fields interacting with scalars in the fundamental representation the Higgs phase is the confining phase. In other words, in certain cases a gauge theory with a spontaneously broken (global) symmetry can be considered as a completely confining theory without symmetry breaking. There is no continuous phase boundary between the confinement and Higgs phase, and a continuous (without phase transitions) passage may occur from one state to another.

The complementarity principle extended to the theory with fermions may result, for instance, in a composite structure of quarks and leptons at the energy scale ~ 1 TeV [7].

The phase structure of Higgs-gauge theories with different symmetry groups is investigated in a number of papers (see, e.g., [8-13]). In most of them the radial mode of the Higgs field is frozen:

$$|\Phi| = 1. \tag{1.1}$$

Studies of the phase structure of Higgs-gauge theories with radially varied scalar fields for Abelian [8,10] and non-Abelian SU(2) symmetries [9] have shown that the form of phase diagrams will essentially change when the assumption (1.1) is rejected.

The present paper is devoted to the study of the phase structure of the theory of SU(2)-gauge fields interacting with Higgs fields. The Higgs fields are considered in the findamental representation with radially varied mode, i.e., $|\Phi| \neq$ const.

Using the Monte-Carlo method and analytic approximations we have investigated the phase structure of our theory for two variants of the radial measure of integration over Higgs fields.

We note that our results somewhat differ from those of ref. [9].

The model we consider is described in the next paragraph; in the third paragraph we give the details of our Monte-Carlo calculations and, finally, we summarize the numerical results and compare them with some mean-field estimates in the fourth paragraph of this paper.

2. THE CHOICE OF THE MODEL

The action for a system of SU(2)-gauge fields and Higgs scalars in the fundamental representation of the gauge group has the form:

$$S = \beta \sum_{\Box} S_{\Box} + \sum_{L} S_L, \tag{2.1}$$

where $S_{\Box} = 1 - 1/2\ \mathrm{Sp}\, U_{\wp}$ with $U_{\wp} = U_{ij}U_{jk}U_{k\ell}U_{\ell i}$ and $U_{ij} = U_L$ is a gauge field defined on the link $L = (i,j)$ which originates from the site labelled by i and ends at site j. The second term in (2.1) is a sum over all links and is of the form:

$$S = \frac{1}{4}\left(\frac{m^2}{2}\Phi_i^*\Phi_i + \lambda(\Phi_i^*\Phi_i)^2\right) + (\Phi_i^*\Phi_i - \mathrm{Re}\,\Phi_i^* U_{ij}\Phi_j). \qquad (2.2)$$

The Higgs field Φ_i is defined at each site i, and Φ_i is a column of two rows. It is convenient to represent the field Φ_i in terms of a pair of variables (R_i, ϕ_i), where $R_i = \sqrt{\Phi_i^*\Phi_i}$ and Φ_i is a unitary 2x2 matrix: $\phi \subseteq SU(2)$. Then the action S_L can be rewritten as

$$S_L = \frac{1}{4}\left(\frac{m^2}{2}R_i^2 + \lambda R_i^4\right) + R_i^2 - R_i R_j \frac{1}{2}\,\mathrm{Sp}\,(\phi_i U_{ij}\phi_j^*)). \qquad (2.3)$$

As a rule, in what follows $m^2 < 0$. The partition function in the model (2.1)-(2.3) has the form

$$Z = \int \prod_i d\mu(R_i)\, d\phi_i \prod_L dU_L\, \ell^{-S}, \qquad (2.4)$$

where dU_L and $d\phi_i$ are Haar's measures on the SU(2) group. The radial measure of integration is to be chosen in accordance with the model. If the radial mode is frozen, as, for instance, in [11-13], then

$$d\mu(R_i) \sim \delta(R_i - 1)\, dR_i\,. \qquad (2.5)$$

In this paper we have chosen the radial phase in two variants:

$$d\mu(R_i) \sim dR_i\,, \qquad (2.6)$$

$$d\mu(R_i) \sim R_i^3\, dR_i\,. \qquad (2.7)$$

The variant (2.7) for $d\mu(R)$ for SU(2)-symmetry group was also used in [9]. The simple choice of the radial mode (2.5) ("frozen radial mode") comes from the belief that in the continuum limit, when the correlation length tends to infinity, fixation of the radial mode in the lattice (bare) action (see (2.5)) is no longer essential. Indeed, as the fixed point of the renormalization group is characteristic only of the very renormalization-group transformation and has nothing to do with the choice of the initial action, it might be assumed that fixation of the radial mode is not very strong constraint. However, it may be true if the theory contains only one fixed point. If, that is more realistic, the theory contains several fixed points, the choice of the bare action (the choice of a point on the canonical sufrace) may turn out to be essential [2].

A different choice of the bare action in the course of studying renormalization-group properties of the theory may result in different fixed points and, consequently, in different physical theories in continuum.

All the aforesaid signifies the necessity of an accurate examination of the problem of choosing the lattice (bare) action for a system of gauge-fields interacting with matter fields and, in particular, the necessity of studying the dependence of the phase structure of the theory on the radial measure.

3. MONTE-CARLO PROCEDURE

The numerical study of the model (2.1)-(2.3) was made by the Monte-Carlo method. All our numerical experiments have been performed on 4^4 - and 6^4-lattice with periodic boundary conditions. According to our calculations the results on 4^4 lattice do not in practice differ from those on 6^4 lattice.

In our calculations we have used the Metropolis algorithm [14].

The order parameters we have used are the mean action per plaquette $\langle S_\square \rangle$ and the mean squared radial part of the Higgs field $\langle R^2 \rangle$.

The Higgs field at each site was renewed in two steps; first the radial part of the field, and then the angular part were changed to new ones. New values of both the scalar and gauge degrees of freedom are accepted or rejected in accordance with the prescription of the Metropolis algorithm.

Foe each change of the field value on a link or at a site 5-10 triels were undertaken. The acceptance rate on the average was about 50%.

The behaviour of order parameters near phase-transition points was investigated by two different techniques:

I. Thermal Cycles

One of the parameters of the model (β or m^2) is gradually varied up to a given value and back. At each intermediate step a given number of iterations is performed starting from the last configuration reached at the preceding step. If the thermal cycle carried the system across a point of phase transition this produces a typical hysteresis loop on the thermal cycle curve for the order parameter.

II. Simulations from Different Types of Initial Configurations (Starts)

a) The start ordered in the radial part of the Higgs field with small values of R_i: $R_i^{(o)} = 0$ at different (ordered or disordered) initial configurations for the angular part of the Higgs field;

b) The start ordered in the radial part with large values of R_i : $R_i^{(0)} \approx 3\div5$ at disordered initial configurations for the angular part of the Higgs fields,etc. The initial configurations of the gauge field were either totally ordered ($U_L = 1$) or totally randomized. The sequence of renewing of variables on links and at sites was chosen in a random way (stochastic sweeps).

4. MONTE-CARLO RESULTS AND THEIR INTERPRETATION

In this section we shall present our results obtained by the Monte-Carlo calculation and compare them with the results of approximate calculations with an effective potential.

All our calculations were carried out for two radial measures: $d\mu(R) \sim dR$, $d\mu(R) \sim R^3\,dR$.

4.1. Radial Measure $d\mu(R) \sim dR$

At $\beta = 0$ and small λ there occurs a first-order phase transition. In Fig.1 we show the thermal cycle over m^2 for the order parameter $\langle R^2 \rangle$ at $\beta = 0$ and $\lambda = 0.1$. That the first-order phase transition does exist can be seen from the dependence of order parameter $\langle R^2 \rangle$ on the iteration number N_{iter} (Fig.1b). At $\beta = 0$, $\lambda = 0.1$, and $m^2 = -5$ two "long-lived" states are observed, one of them being stable and the other metastable.

If we consider analytic continuation in β to negative values we shall observe that the characteristic hysteresis loop gradually shrinks to vanish completely for $\beta = -3$ ($\lambda = 0.1$). At that point the dependence of $\langle R^2 \rangle$ on m^2 has a sharp break for $m^2 \approx -6.25$ (see Fig.2a). With further decreasing β this break gets smoothing. From Fig.2b it is seen that when $\beta = -\infty$ the dependence of $\langle R^2 \rangle$ on m^2 is smooth enough.

Thus, we observe that the curve of first-order phase transitions in the (m^2, β)-phase plane has an end point that may be interpreted as a point of the second-order phase transition.

For positive values of β up to infinite the behaviour of the order parameter $\langle R^2 \rangle$ testifies to the existence of first-order phase transitions. In Fig.3a we present the values of Monte-Carlo calculations obtained in the thermal cycle over m^2 at $\beta = \infty$; $\lambda = 0.1$; and in Fig.3b, the dependence of $\langle R^2 \rangle$ on the iteration number at $\beta = \infty$; $m^2 = -3.7$, $\lambda = 0.1$ for two different starts. When $\beta = \infty$ the phase transition occurs at $m^2 \approx -3.57$ ($\lambda = 0.1$). The final shape of phase-transition curves at different λ is plotted in Fig.4.

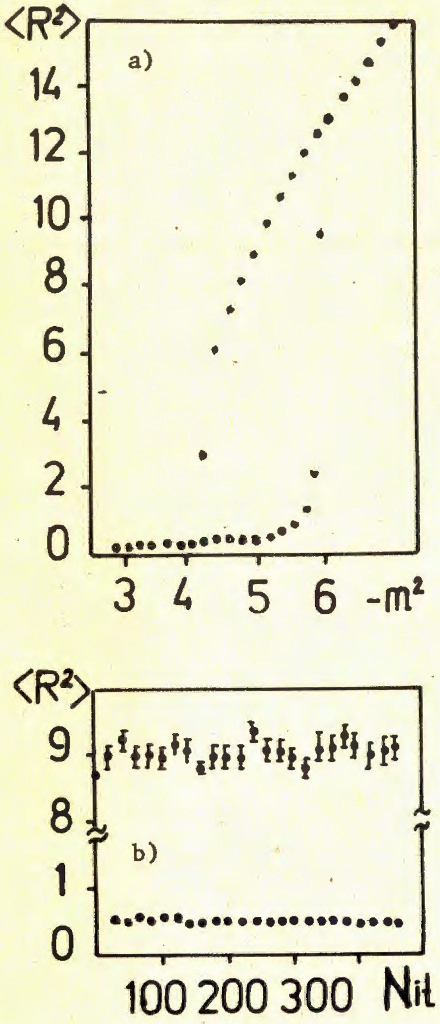

Fig.1. a) Thermal cycle in m^2 for $\beta = 0$, $\lambda = 0.1$. b) The dependence of the order parameter $\langle R^2 \rangle$ on the iteration number N_{iter} for $\beta = 0$; $\lambda = 0.1$; $m^2 = -5$.

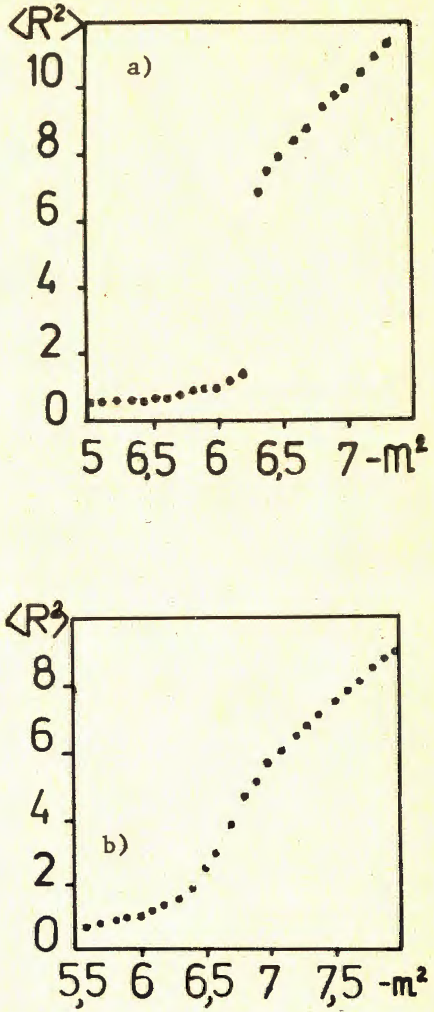

Fig.2. a) m^2-dependence of $\langle R^2 \rangle$ for $\beta \approx -3$; $\lambda = 0.1$. b) m^2-dependence of $\langle R^2 \rangle$ for $\beta = -\infty$; $\lambda = 0.1$.

Solid curves represent first-order phase transitions for different λ and these curves have endpoints.

With increasing λ the curve is shifted to the right and upward on the phase plane.

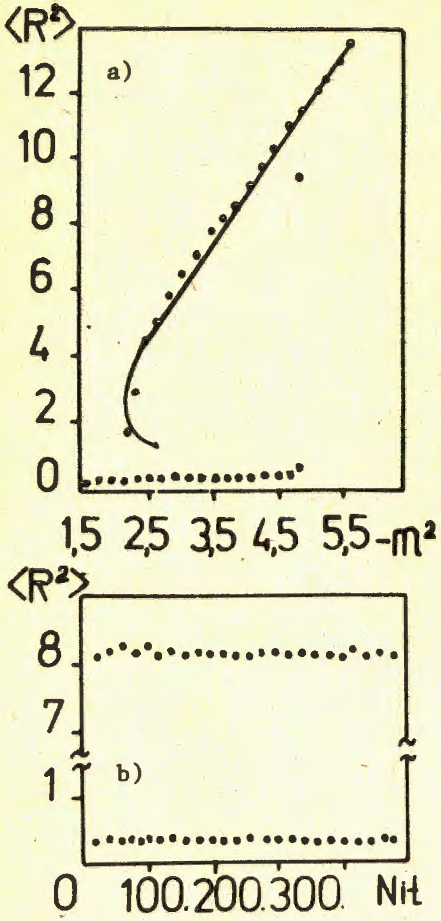

Fig.3. a) Thermal cycle in m^2 for $\beta=\infty$; $\lambda = 0.1$. Continuous line is obtained from effective potential (4.6). b) The dependence of $\langle R^2 \rangle$ on the iteration number for $\beta=\infty$; $m^2 \approx -3.7$; $\lambda = 0.1$.

Fig.4. Phase diagram in the (m^2 , $\frac{2}{\pi}$ arctg β)-plane for different λ. Continuous lines correspond with first-order phase transition lines.

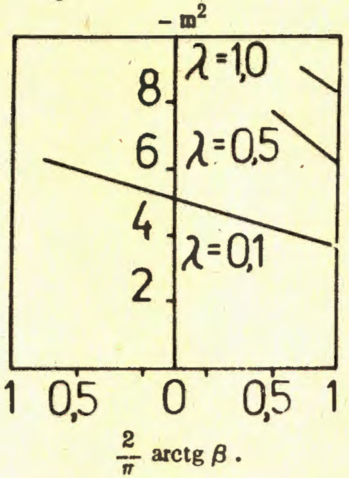

The nature of phase transitions can be understood from an approximate calculation of the effective potential V_{eff} .

At $\beta = 0$ the integration over gauge fields U_{ij} can be carried out exactly, and as a result the partition function becomes

$$Z = \int \prod_i d\mu(R_i)\, e^{-\sum_{ij} S_{ij}} \quad . \tag{4.1}$$

The action S_{ij} depends now only on the radial variables of the Higgs field R_i :

$$S_L = S_{ij} = (1+\frac{m^2}{8}) R_i^2 + \frac{\lambda}{4} R_i^4 - \ln W(R_i R_j),$$

$$W(z) = \frac{2}{z} I_1(z), \tag{4.2}$$

and I_1 is a modified Bessel function.

With the help of action (4.2) we obtain in the lowest approximation (see [15]) the following expression for the effective potential*:

$$V_{eff} = (1+\frac{m^2}{8})\tilde{R}^2 + \frac{\lambda}{4}\tilde{R}^4 - \ln W(\tilde{R}^2), \tag{4.3}$$

where $\tilde{R} = \langle R \rangle$.

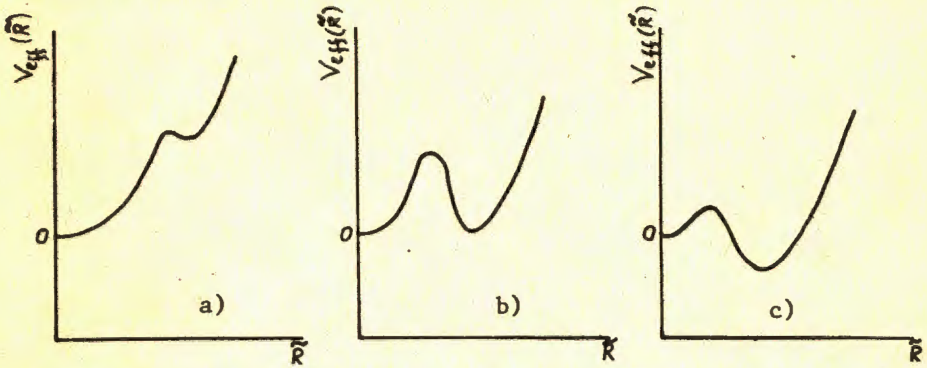

Fig.5. The qualitative dependence of effective potential $V_{eff}(\tilde{R})$ for $\beta = 0$, sufficiently small λ, and different values m^2 a) $|m^2| < |m_c^2|$; b) $m^2 = m_c^2$; c) $|m^2| > |m_c^2|$.

At λ small enough expression (4.3) may have two minima, one of them being at zero. At values of $|m^2|$ smaller than some "critical" value of $|m_c^2|$ the minimum at zero is below the other minimum and corresponds to a stable phase, whereas the second to a metastable phase (Fig.5a). At $m^2 = m_c^2$ the value of V_{eff} at both the minima equals zero (Fig.5b), and for $|m^2| > |m_c^2|$ the second minimum corresponds to the stable phase, whereas the first one to a metastable (Fig.5c). Thus, the point $m^2 = m_c^2$ is the point of first-order phase transition.

Formula (4.3) gives for the phase transition at $\lambda = 0.1$, $m^2 = -5$, that is in good agreement with the Monte-Carlo calculations. And what is more, this formula provides also a good numerical agreement for the order parameter $\langle R^2 \rangle$ in both the upper and lower phase of the hysteresis loop (Fig.1a). With increasing λ the magnitude of the jump of the order parameter calculated by (4.3) becomes decreasing and at $\lambda \approx 0.5$ ($\beta = 0$)

---

* Really the effective potential must be apparantly a convex one (see, for instance 16-18)). But the definition of V_{eff} we have used (15) is absolutely noncontradictory for the lowest approximation and is more convenient for calculations.

it vanishes. The effective potential V_{eff} here can no longer have a two-minimum structure: for $|m^2|<|m_c^2|$ the only minimum of V_{eff} is at zero, and for $|m^2|>|m_c^2|$ it is not at zero (Fig.6). This situation is characteristic of a second-order phase transition. When $\lambda > 0.5$, the effective potential (4.3) testifies to no phase transitions (at $\beta = 0$). This λ-dependence is in good agreement with the one obtained by Monte-Carlo calculations (Fig.6).

When $\beta = \infty$, all the gauge fields may be replaced by unity, however, in this case one can no longer remove the integration over angular variables of the Higgs field and thus reduce the problem to the calculation of the effective potential over the radial variable R.

Nevertheless, one may calculate the effective potential as a function of averages of real and imaginary parts of the Higgs-field components $\Phi_i^{(a)}$, where

$$\Phi_i^{(1)} = \mathrm{Re}(\Phi_i)_1, \quad \Phi_i^{(2)} = \mathrm{Im}(\Phi_i)_2, \quad \Phi_i^{(3)} = \mathrm{Re}(\Phi_i)_2, \quad \Phi_i^{(4)} = \mathrm{Im}(\Phi_i)_2,$$

and from the behaviour of the effective potential guess the dependence V_{eff} on $\langle R \rangle$.

The partition function Z for $\beta = \infty$ can be represented in the form

$$Z = \int \prod_i \prod_{a=1}^{4} d\Phi_i^{(a)} \, e^{-\tilde{S}(\Phi)}, \qquad (4.4)$$

where

$$\tilde{S}(\Phi) = \sum_i \Big[\sum_0 (\Phi_i^* \Phi_i - \mathrm{Re}\, \Phi_i^* \Phi_{i+\mu}) + V(R_i) \Big],$$
$$V(R_i) = \frac{m^2}{2} R_i^2 + \lambda R_i^4 + \frac{3}{2} \ln R_i^2 . \qquad (4.5)$$

The effective potential in the lowest approximation following from (4.5) is of the form

$$V_{eff}(\tilde{R}) = \frac{m^2}{2} \tilde{R}^2 + \lambda \tilde{R}^4 + \frac{3}{2} \ln \tilde{R}^2 , \qquad (4.6)$$

where $\tilde{R} = \sqrt{\sum_{a=1}^{4} (\tilde{\Phi}^{(a)})^2}$, $\quad \tilde{\Phi}^{(a)} = \langle \Phi_i^{(a)} \rangle$.

The effective potential (4.6) turns to minus infinity as $\tilde{R} \to 0$ and may possess a local minimum at nonzero $\tilde{R}$. The value of m^2 at which this local minimum appears is determined from the equation

$$\frac{dV_{eff}}{d\tilde{R}^2} = 0 . \qquad (4.7)$$

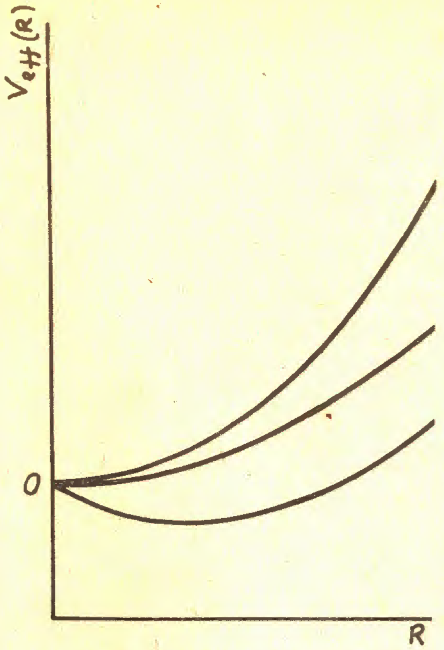

Fig.6. Qualitative dependence of V_{eff} for $\lambda \approx 0.5$, $\beta = 0$, and different values m^2.

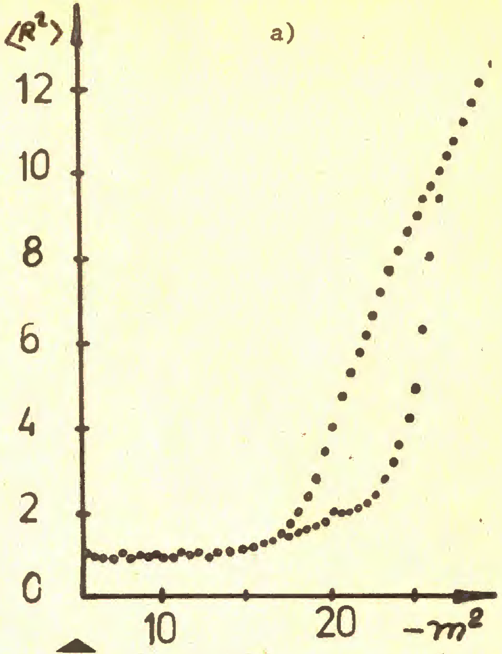

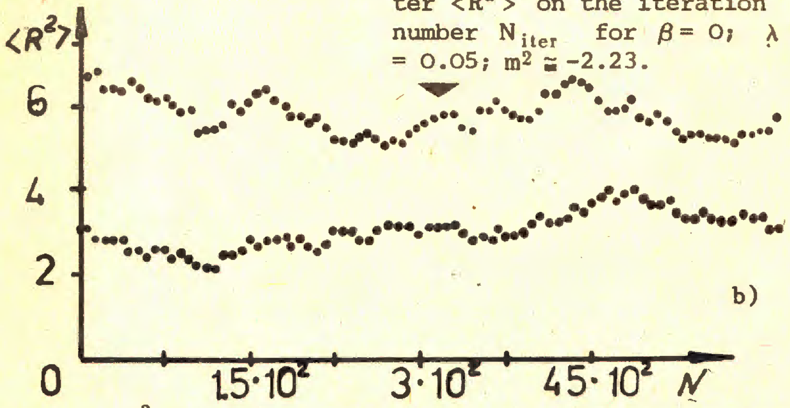

Fig.7. a) Thermal cycle in m^2 for $\beta = 0$, $\lambda = 0.05$. b) The dependence of the order parameter $\langle R^2 \rangle$ on the iteration number N_{iter} for $\beta = 0$; $\lambda = 0.05$; $m^2 \cong -2.23$.

The value of m^2 determined from (4.7), at which nonzero local minimum appears, equals approximately $m^2 \approx -2.2$ ($\lambda = 0.1$) and is in good agreement with the value at which the hysteresis loop starts, calculated by the Monte-Carlo method (see Fig.3a). The value of $\tilde{R}^2$ as a function of m^2 corresponding to the location of that minimum of the effective potential (4.6) almost coincides with the upper branch of the hysteresis loop in Fig.3a constructed for the order parameter $\langle R^2 \rangle$.

4.2. Measure $d\mu(R) \sim R^3 dR$

When the radial mode is defined by (2.7), the phase diagram differs noticeably in form from the one for the radial mode (2.6). At finite β and λ small enough the first order phase transition is also observed in this case. In Fig.7a,b we draw the hysteresis loop versus m^2 at $\beta = 0$, $\lambda = 0.05$ and the dependence of the order parameter $\langle R^2 \rangle$ on the iteration number N_{it} at $\beta = 0$, $\lambda = 0.05$, $m^2 = -2.23$. With growing λ the hysteresis loop gets narrowing and then disappears at $\lambda = 0.1$ and $\beta = 0$ (Fig.8a)- whereas at $\lambda = 0.1$, $\beta = 1$ it is still present (Fig.8b). This picture is in good agreement with predictions obtained in the lowest approximation for the effective potential.

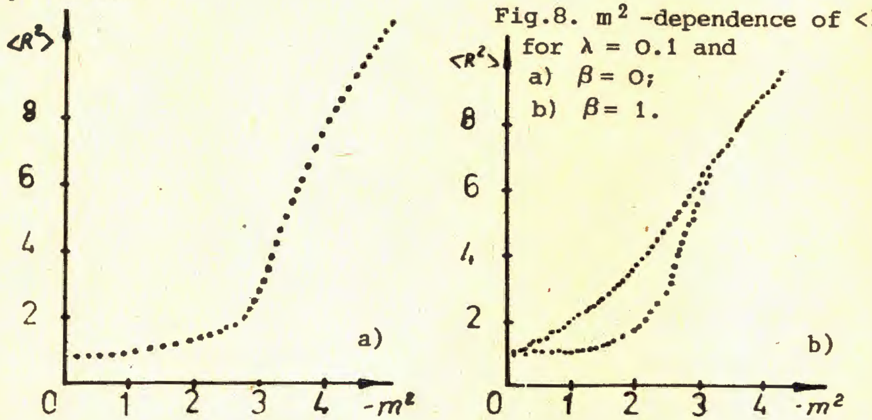

Fig.8. m^2-dependence of $\langle R^2 \rangle$ for $\lambda = 0.1$ and
a) $\beta = 0$;
b) $\beta = 1$.

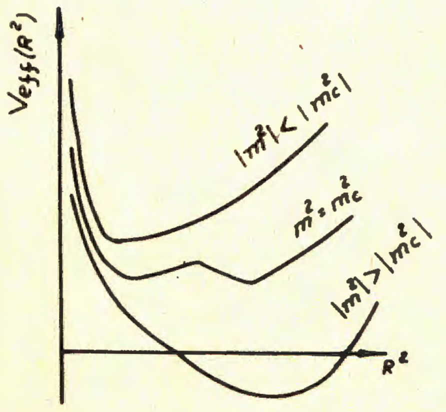

Fig.9. Qualitative dependence of V_{eff} for $\lambda = 0.05$, $\beta = 0$ and different values m^2.

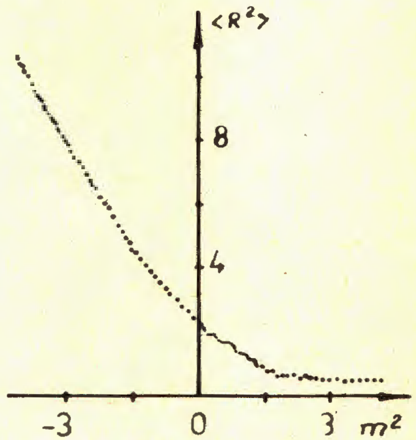

Fig.10. The dependence of the order parameter $\langle R^2 \rangle$ on m^2 for $\beta = 0$, $\lambda = 0.1$.

Following the procedure described in sect.4.1, it is easy to find the effective potential at $\beta = 0$ in the lowest approximation in the form:

$$V_{eff} = (1 + \frac{m^2}{8}) \tilde{R}^2 + \frac{\lambda}{4} \tilde{R}^4 - \ln \frac{2I_1(\tilde{R}^2)}{\tilde{R}^2} - \frac{3}{2} \ln \tilde{R}^2 . \qquad (4.8)$$

In Fig.9 we show a qualitative dependence of $V_{eff}(R)$ for different masses at $\lambda = 0.05$ and $\beta = 0$.

That the effective potential has two minima points to the presence of a first-order phase transition (cf.sect.4.1). With growing λ there are no two minima of V_{eff} for any m^2, and the first-order phase transition vanishes.

When β is growing and λ is fixed, the hysteresis loop becomes narrowing and then disappears. In Fig.10 $\langle R^2 \rangle$-dependence of m^2 is shown for $\beta = \infty$ and $\lambda = 0.1$. There is no hysteresis loop, and at positive m^2 a sharp break occurs in the behaviour of $\langle R^2 \rangle$. From considerations based on the calculation of the effective potential (cf,sect.4.1) it follows that this point may be identified with the second-order phase transition.

The phase diagram for the SU(2) gauge-Higgs model with the radial measure (2.7) is similar in form to the one plotted in Fig.4.

In the (m^2, β) phase plane at λ fixed there is a curve of phase transitions with the left end point that may be identified with the second-order phase transition. At finite β ($\beta < \infty$) each point of the curve corresponds to a first-order phase transition. When $\beta \to \infty$, the first-order phase transition disappears, and the curve of the m^2-dependence of $\langle R^2 \rangle$ for m^2 positive gets a sharp break which may represent the second-order phase transition. With increasing λ the curve of phase transitions shifts to the right and upwards.

5. CONCLUSION

We have analysed the phase structure of the lattice SU(2) gauge-Higgs theory, and Higgs fields are allowed to vary radially.

Our Monte-Carlo calculations are in good agreement with approximate calculations with an effective potential.

We have used two different radial measures for scalar fields.

Main conclusions are as follows.

The radial mode of Higgs fields affects the whole structure of the theory.

Phase diagrams (the order of phase transitions their position on the phase plane) depend crucially on the choice of radial measure.

At present it is difficult to answer the question of which of the critical points we have observed may correspond to the continuum limit of the theory. This requires further studies.

At the same time in both the models we have considered the curves of phase transitions do not divide the whole phase plane into two separate parts: this means that there exists a region of analyticity, where one can pass from one phase (say, below the line of phase transitions) to another (above that line) without jump of the order parameters or its derivatives. This is an argument in favour of the complementarity principle.

In conclusion we would like to thank N.N.Govorun, V.A.Matveev, T.Margaritis, M.G.Meshcheryakov, V.A.Meshcheryakov, D.V.Shirkov, A.N.Sissakian, K.Szlachanyi for useful discussion and interest in the work.

REFERENCES

1. Wilson K.G. Phys.Rev., 1974, D14, p.2445.
2. Wilson K.G., Kogut J.B. Phys.Rep., 1974, C12, p.75.
3. Brezin E., Drouffe J.M. Nucl.Phys., 1982, B200, p.93.
4. Pena A., Sokolovsky M. Phys.Lett., 1984, B134, p.99.
5. Fradkin E., Shenker S.H. Phys.Rev., 1979, D19, p.3682.
6. Farhi E., Susskind L. Phys.Rep., 1981, 74, p.277.
7. Dimopoulos S., Raby S., Susskind L. Nucl.Phys., 1980, B173, p.208.
8. Munehisa T., Munehisa Y. Phys.Lett., 1982, B116, p.363; Munehisa T., Munehisa Y. Nucl.Phys., 1983, B215, p.508. Munehisa Y. FNAL Preprint 84/31-T, 1984.
9. Kuhnelt H., Lang C.B., Vones G. Nucl.Phys., 1984, B230, p.16.
10. Gerdt V.P., Ilchev A.S., Mitrjushkin V.K. JINR, E2-83-758, Dubna, 1983.
11. Mack G., Meyer H. Nucl.Phys., 1982, B200, p.249.
12. Lang C.B., Rebbo C., Virasoro M. Phys.Lett., 1981, B104, p.294.
13. Creutz M. Phys.Rev., 1980, D21, p.1006.
14. Metropolis N. et al. J.Chem.Phys., 1953, B21, p.1087.
15. Coleman S., Weinberg E. Phys.Rev., 1973, D7, p.1888.
16. Callaway D.J.E., Carson L.J. Phys.Rev., 1982, D25, p.531.
17. Callaway D.J.E., Maloof D.J. Phys.Rev., 1983, D27, p.406.
18. Fujimoto Y., O'Raifeartaigh L., Parravicini G. Nucl.Phys., 1983, B212, p.268.

Received by Publishing Department
on May 4, 1984.

Гердт В.П. и др. E2-84-313

Фазовая структура SU(2)-симметричной хиггс-калибровочной теории на решетке

В работе методом Монте-Карло, а также с помощью приближенного вычисления эффективного потенциала исследуется фазовая структура SU(2)-симметричной хиггс-калибровочной теории. Хиггсовские поля рассматриваются в фундаментальном представлении, и радиальная мода хиггсовских полей разморожена. Рассматриваются два различных способа размораживания радиальной моды. Построены фазовые диаграммы теории, а также показано, что вид фазовой диаграммы сильно зависит от способа размораживания радиальной моды.

Работа выполнена в Лаборатории теоретической физики ОИЯИ.

Препринт Объединенного института ядерных исследований. Дубна 1984